Mechanics & Industry 14, 431–439 (2013)

DOI: 10.1051/meca/2013084
www.mechanics-industry.org

Mechanics & Industry

Artificial neural networks back propagation algorithm for cutting force components predictions

Issam Hanafi[1,a], Francisco Mata Cabrera[2], Abdellatif Khamlichi[3], Ignacio Garrido[2] and José Tejero Manzanares[2]

[1] Ecole Nationale des Sciences Appliquées d'Al Hoceima (ENSAH), BP 03 Ajdir, 32000 Al Hoceima, Morocco
[2] University Polytechnic School Of Mining and Industrial Engineering of Almaden, 1 Plaza Manuel Meca, 13400 Almaden, Spain
[3] Faculty of Sciences at Tetouan, BP 2121 M'hannech, 93002 Tetouan, Morocco

Received 28 January 2013, Accepted 11 December 2013

Abstract – Reinforced Poly Ether Ether Ketone with 30% of Carbon Fiber (PEEK CF30) offer several thermo-mechanical advantages over standard materials and alloys which make them better candidates in different applications. However, the hard and abrasive nature of the reinforcement fiber is responsible for rapid tool wear and high machining costs. It is very important to find highly effective ways to machine that material. Accordingly, it is important to predict forces when machining fiber matrix composites because this will help to choose perfect tools for machining and ultimately save both money and time. In this study, Artificial Neural Network (ANN) was applied to predict the cutting force components in turning operations of PEEK CF30 using TiN coated cutting tools under dry conditions where the machining parameters are cutting speed ranges, feed rate, and depth of cut. For this study, the experiments have been conducted using full factorial design experiments (DOEs) on CNC turning machine. The results indicated that the well-trained (ANN) model could be able to predict the cutting force components in turning of Carbon Fiber Reinforcement Polymer (CFRP) composites. Complementary results that were not used during derivation of the ANN model have enabled one to assess the validity of the obtained predictions.

Key words: Neural Network / modeling / machining / PEEK CF30 / TiN coated inserts / radial force / cutting force / feed force

1 Introduction

Cutting forces are the background for the evaluation of the necessary power in machining. They are also used for dimensioning of machine tool components and the tool body. They influence the deformation of the work piece machined, its dimensional accuracy, chip formation, and machining system stability. During the cutting process, the work piece acts on the tool with a certain force whose decomposition in three directions can be used as a basis for the definition of cutting forces [1]. A considerable amount of investigations has been directed towards the prediction and measurement of cutting forces. That is because the cutting forces generated during composites cutting have a direct influence on the generation of heat and thus tool wear, quality of machined surface and accuracy of the work piece. The machining of fiber-reinforced materials requires special considerations about the wear resistance of the tool. High speed steel (HSS) is not suitable for cutting owing to the high tool wear and poor surface finish. Hence, carbide and diamond tools are used as suitable cutting tool materials [2]. Konig et al. [3] found that measurement of surface roughness in fiber reinforced plastics is less dependable than in metal, because protruding fiber tips may lead to incorrect result or at least large variation of the reading. Kevlar fiber reinforced plastics (KFRP) machined surface exhibit poor surface finish due to the fussiness caused by delaminated, dislocated and strain ruptured tough Kevlar fibers. Cabrera et al. [4] investigated the machinability in turning process of carbon fibers reinforced plastics (CFRP) using polycrystalline diamond (PCD) and cemented carbide tool (K10). Two parameters such as cutting speed and feed rate were selected. It was observed that the polycrystalline diamond provides a better machinability index in comparison to cemented carbide tool (K10). Hussain et al. [5] developed a surface roughness and cutting force prediction model for the machining of GFRP tubes by using a carbide

[a] Corresponding author: hanafi.issam@yahoo.fr

tool (K20), a cubic boron nitride (CBN) and a polycrystalline diamond (PCD) using Response Surface Methodology (RSM). Four parameters such as cutting speed, feed rate, depth of cut and work piece were selected. It was found that the polycrystalline diamond (PCD) cutting tool was better than other two tools used.

Due to the complex tool configurations/cutting conditions of metal cutting operations and some unknown factors and stresses, theoretical cutting force calculations failed to produce accurate results. Also the experimental studies are expensive and time consuming. More over, their results are valid only for the experimental conditions used and depend greatly on the accuracy of calibration of the experimental equipments and apparatus used [6]. Therefore, modelling the experimental measurement of the cutting forces became unavoidable.

A mechanics model was developed for predicting the forces when machining aluminum alloy based MMCs reinforced with ceramic particles. A comparison between predicted and experimental force results showed excellent agreement [7]. An experimental and numerical study is performed to determine the cutting forces and their variation with depth of cut, tool rake angle in Unidirectional Glass Fiber Reinforced Plastics (UD-CFRP), and Unidirectional Carbon Fiber Reinforced Plastics (UD-GFRP) with fiber orientation varying between 15° and 90° with an increment of 15° with respect to cutting direction [8]. The micromechanical finite element model was a better representation of the material for cutting process as compared to an Equivalent Homogenous Material (EHM) model as it explains the mechanism of machining. It provides a good agreement with the experimental cutting and thrust forces for both the material system investigated.

Chip tool interface friction in machining of Al/SiCp composites has been considered to involve two-body abrasion and three-body rolling caused due to presence of reinforcements in composites. The model evaluates resulting coefficient of friction to predict the cutting forces during machining of Al/SiCp composites using theory of oblique cutting [9].

A methodology has been presented for simulating helical end milling of fiber reinforced polymer composites [10]. The methodology utilizes mechanistic modeling approaches from metal cutting and the transformation of specific cutting energy data from orthogonal cutting to oblique cutting. The helical end mill is treated as a stack of finite thickness disks with oblique cutting edges. The cutting forces for each disk are calculated using the mechanistic and transformation techniques from metal cutting, and the overall cutting forces are calculated by the sum of the contributions of all disks.

An analytical approach to determine the cutting forces generated during machining of metal matrix composite. The presented model accounts for the particle fracture and particle contribution to the friction force generated along the chip tool interface, The results show acceptable agreement between the theoretically predicted and experimentally measured cutting forces [11]. The Johnson-Cook model [12] was utilized to account for the temperature, high strain rate, and high strain generated during machining. Predicted forces show good agreement with the measured force as well under different cutting conditions such as speed, depth of cut, and feed rate.

Tsao and Hocheng [13] have established the relationship between the input parameters feed rate, spindle speed, and drill diameter; with the output parameters thrust force and surface roughness in drilling composite laminates. They have used radial basis function network for the prediction. Mishra et al. [14] have predicted the tensile strength of the unidirectional glass fiber reinforced polymer composites. They have considered the input parameters as feed rate, drill point geometry and spindle speed. They have generated the database by drilling the composite materials at different input conditions.

A fuzzy rule-based model is developed to predict the machining force components in turning of carbon fibre-reinforced polymer (CFRP) [15]. Good agreement is observed between the predictive model results and the experimental values.

The machining process is very complex and analytical models fail to give consistent accurate predictions of machining criteria. Traditional methods such as statistical regression and response surface methodology (RSM) approaches have been used by some researchers in modeling the turning process. But these methods cannot adequately recover the nonlinear relationships between cutting conditions and the output responses. Through massive parallelization to solve complex nonlinear problems, artificial neural networks (ANN) models, are expected to be more suitable.

The present article deals with the determination of the cutting force components in turning of PEEK CF30 composite by using TiN coated cutting tools, when different levels of the cutting parameters are used. The proposed models for cutting force components were experimentally derived with the use of an artificial neural network back propagation algorithm analysis, and they were developed mutually. The use of experimental data that is able to cover the turning process and provided the validated model. The experimental and predicted results have a close relationship with each other, which indicates that the neural network can be applied for the prediction of cutting force components in turning of CFRP composites.

2 Experimental work

The work material used for the present investigation was reinforced PEEK composite with 30% of fiber carbon (PEEK CF30) manufactured by ERTA® cylindrical work pieces with 50 mm in diameter and a length of 100 mm. Fiber orientations were unidirectional parallel (0°) to the axis of the tube. Dry turning experiments were carried out on a GORATU G CRONO 4S CNC of 26.5 KW spindle power and maximum spindle speed 3350 rpm using TiN coated ISCAR WNMG 080408-TF cutting tools. They were mounted on A SDJCL 2020 K11 tool holder. Three component turning forces (radial force Fp, cutting force

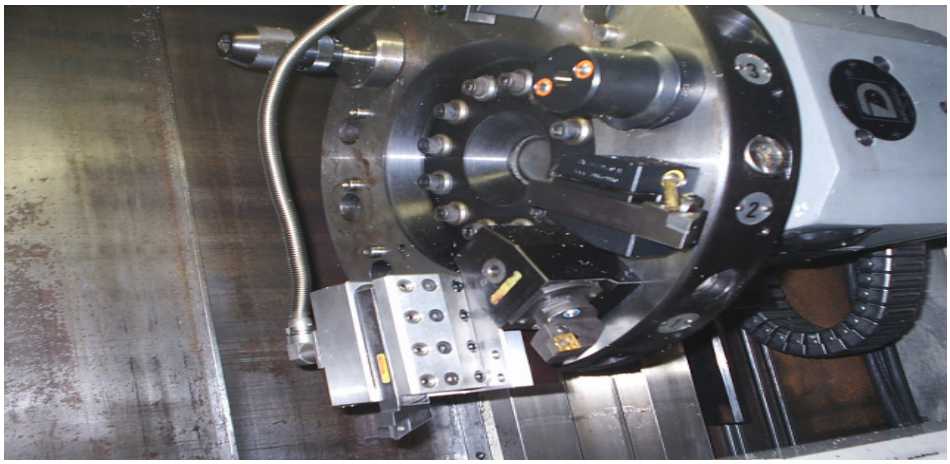

Fig. 1. Kistler piezoelectric dynamometer used to measure cutting forces.

Table 1. Mechanical and thermal properties of PEEK CF30 composite.

Mechanical and thermal properties	PEEK CF30	Unit
Tensile modulus	7700	MPa
Tensile strength	130	MPa
Melting temperature	340	°C
Density	1.41	$g.cm^{-3}$
Coefficient of thermal expansion for temperature less than 150 °C	25×10^{-6}	$m.m^{-1}.K^{-1}$
Coefficient of thermal expansion for temperature exceeding 150 °C	55×10^{-6}	$m.m^{-1}.K^{-1}$

Table 2. Machining parameters and their considered levels.

	Level	Code
Cutting speed ($m.min^{-1}$)	300	1
	200	2
	100	3
Feed rate ($mm.rev^{-1}$)	0.20	1
	0.15	2
	0.05	3
Depth of cut (mm)	1.5	1
	0.75	2
	0.25	3

Fc, and feed force Fa) were recorded with a Kistler piezoelectric dynamometer model 9121 connected to a load amplifier and data acquisition board, as shown in Figure 1. The mechanical and thermal properties of work material given by the manufacturer are summarized in Table 1.

The experiments were conducted according to a full factorial Design of Experiment (DOE) table using the Taguchi approach [16]. The three cutting parameters selected for the present investigation are: cutting speed (v), feed rate (f) and depth of cut (d). The other parameters, which relate to the mechanical and geometrical properties such as thickness of the workpiece are not considered in this work. Since the considered variables are multi-level and their outcome effects are not linearly related, it has been decided to use three level tests for each factor. The machining parameters used, and their levels are given in Table 2.

According to performed preliminary tests, the temperature reached has not produced any significant changes in the surface finish and tool wear, even during dry turning of PEEK CF30 with the highest cutting speed and specific cutting pressure ranges. The maximum reached temperature was well below the heat resistance temperature which is for PEEK about 250 °C. This experimental evidence proved that, for the specific tested range of parameters, there would be no need to use any coolant. Moreover, using a coolant during machining of PEEK is inadvisable as the risk of its absorption exists, which could result in some dimensional instability [17].

In developing mathematical models that can be effectively identified from experimental data, careful planning of the experimentation is needed. Hence, it is essential to have a well designed set of experiments. This can substantially reduce the number of tests required to be performed; as compared with empirical experimental approaches which consist only in collecting data without performing any design of experiment a priori, or "one change at a time" experimental methods, it allows a judgment on the significance to the output of input variables acting alone, as well input variables acting in combination with one another. "One change at a time" testing always carries the risk that the experimenter may find one input variable to have a significant effect on the response while failing to discover that changing another variable may alter the effect of the first. Among the methods that can be used to achieve a rational Design Of Experiment (DOE), Taguchi method which is based on statistical techniques

Table 3. Experimental lay out and results used for training the network.

Exp. No.	Vc (m.min^{-1})	d (mm)	f (mm.rev^{-1})	Radial force Fp (N)	Cutting force Fc (N)	Feed force Fa (N)
1	300	1.5	0.2	74.97	107.79	101.11
2	300	1.5	0.15	64.31	96.00	85.13
3	300	1.5	0.05	45.90	76.17	42.00
4	300	0.75	0.2	77.80	53.46	59.94
5	300	0.75	0.15	86.74	58.39	56.74
6	300	0.75	0.05	59.70	47.41	28.36
7	300	0.25	0.2	72.74	23.17	28.44
8	300	0.25	0.15	70.33	23.89	26.22
9	300	0.25	0.05	49.26	18.49	15.74
10	200	1.5	0.2	111.18	133.03	107.79
11	200	1.5	0.15	101.55	125.55	93.42
12	200	1.5	0.05	68.78	98.65	47.91
13	200	0.75	0.2	111.39	76.28	68.68
14	200	0.75	0.15	100.93	70.93	57.69
15	200	0.75	0.05	68.47	53.99	30.85
16	200	0.25	0.2	85.42	28.75	33.57
17	200	0.25	0.15	78.08	26.65	29.37
18	200	0.25	0.05	56.54	20.48	17.47
19	100	1.5	0.2	121.14	145.49	118.21
20	100	1.5	0.15	112.73	136.84	101.71
21	100	1.5	0.05	78.02	104.19	52.19
22	100	0.75	0.2	98.43	66.91	54.20
23	100	0.75	0.15	102.63	67.71	56.97
24	100	0.75	0.05	98.95	67.42	53.78
25	100	0.25	0.2	91.84	28.43	36.19
26	100	0.25	0.15	86.60	27.19	31.93
27	100	0.25	0.05	66.45	21.94	20.72

is commonly utilized. Here the particular case of a full factorial DOE table will be employed.

The experimental layout plan, performed according to a full factorial DOE table and which included 27 combinations, is given in Table 3. It should be mentioned that the cutting force considered in this work means an average value obtained through a sampling rate at 10 000 Hz. Every test was repeated four times to detect any extraordinary variability. The tests were all reproducible [18].

3 Derivation of ANN based models

An artificial neural network is a parallel distributed information processing system. It stores the samples with distributed coding, thus forming a trainable nonlinear system. The main characteristic of a neural network approach is its functions like the human brain. Given the input and the expected outputs, the program has the ability of being self adaptive to the environment so as to respond to different inputs rationally [17].

Basically, a neural network consists of a number of processing elements linked together via weighted and directed connections. Common configurations of neural networks are fully interconnected. Each processing element receives input signals via weighted incoming connections and then fans out an output signal along connections to each of the other processing elements. The output signal of an element depends on the threshold specified and the transfer function. There are many neural network models which attempt to simulate various aspects of intelligence. Two types of learning are supervised and unsupervised learning. For supervising learning, a set of training input data with a corresponding set of output data is trained to adjust the weights in a network. For unsupervised learning, a set of input vectors is proposed, but no target vectors are specified [18]. To solve the parameter design problems with multiple responses, back-propagation neural networks are applied to construct the functional relationship between control factors and cutting force components, this algorithm consists of the 10 steps described below:

- Step 1: Decide the number of hidden layers.
- Step 2: Decide the number of neurons for the input layer and the output layer. For the input layer, the number of neurons is equal to the number of input variables and for the output layer it is equal to the number of outputs required. Set small number of neurons for the hidden layer.
- Step 3: Get the training input pattern.
- Step 4: Assign small weight values for the neurons connected in between the input, hidden and output layers.
- Step 5: Calculate the output values for all the neurons in hidden and output layers using the following formula.

$$out_j = f\left(net_j\right) = f\left(\sum\nolimits_i w_{ij}\ out_i\right) \qquad (1)$$

where out_i is the output of the ith neuron in the layer under consideration; out_j is the output of the jth neuron in the preceding layer, f is the sigmoid function commonly utilized in engineering problems it has simple derivative and the implementation of back-propagation system is much easier, and can be written as:

$$f\left(net_j\right) = \frac{1}{1 + \mathrm{e}^{\left(-net_j - \theta_j\right)/\theta_0}} \tag{2}$$

where θ_j is a threshold value for j node and parameter θ_0 is used to arrange the form of sigmoid function.

– Step 6: Determine the output at the output layer and compare those with the desired output values. Determine the error of the output neurons.

$$\text{error} = \text{desired output} - \text{actual output}$$

Similarly, determine the root mean square error value of the output neurons

$$Ep = \frac{1}{2}\sum\left(t_{pj} - d_{pj}\right)^2 \tag{3}$$

where Ep is the error for the pth presentation vector, t_{pj} is the desired value for the jth output neuron and d_{pj} is the desired output of the jth output neuron.

– Step 7: Determine the error available at the neurons of the hidden layer and back-propagate those errors to the weight values connected in between the neurons of the hidden layer and input layer. Similarly, back-propagate the errors available at the output neurons to the weight values connected in between the neurons of the hidden layer and output layer using the following formula

$$error\ \delta_{pi} = \left(t_{pi} - d_{pi}\right) d_{pi}\left(1 - d_{pi}\right) \text{ for output neurons} \tag{4}$$

$$error\ \delta_{pi} = \left(t_{pi} - d_{pi}\right) d_{pi}\sum\delta_{pi} W_{ki} \text{ for hidden neurons} \tag{5}$$

Weight adjustment is made as follows:

$$\Delta W_{ji}\left(n = 1\right) = \eta\left(\delta_{pi}\ d_{pi}\right) = \alpha\Delta W_{ji}\left(n\right) \tag{6}$$

where η is the learning rate parameter and α is momentum factor.

– Step 8: Go to Step 3 and do the calculations up to Step 7.
At the end of cycle determine the root-mean-square error value, mean percentage of error and worst percentage of error over the complete patterns. To reach Step 9 check whether it is of reasonable error or not, if so, go to Step 9 otherwise go to Step 3 and repeat Steps 3 to 7.

– Step 9: Stop the iteration and note the final weight values attached to the hidden layer neurons and also to the output layer neurons.

– Step 10: Testing neural network model with the trained weight values, determine the output for the testing pattern and check whether the deviation from desired value is reasonably less or not. If no, try the back propagation with a revised network by changing the number of neurons, altering the learning rate parameters, altering momentum value and altering temperature values.

In the present problem, the back-propagation network consists of three input neurons corresponding to cutting speed, depth of cut and feed rate, three output neurons corresponding to cutting force components (Fc, Fp, Fa).

The neural networks model for the cutting force components prediction was trained according to the following training procedure. In the training process, the trial-and-error method is employed to determine the number of hidden layers, the neurons in each hidden layer, the learning rate, and the momentum factor in the neural networks model. A few neural network structures with varied numbers of hidden neurons were compared. The structure of 3-10-3 neurons was found to yield the least prediction errors and was selected as the system best suited model. Figure 2 shows the architecture of the obtained ANN model.

By following the same trial-and-error procedure, the learning rate was set at 0.7 and the momentum factor at 0.7.

Samples obtained at the experimental stage were randomly divided into three groups to train (70% of the samples), validate (15% of the samples) and test (15% of the samples).

Validation samples were used to measure network generalization and stop the training when the generalization stopped improving. Testing samples have no effect on training and so provide an independent measure of a network's performance. The back-propagation algorithm automatically stops training when generalization ceases to improve, as an increase in the root mean square error (RMS) of the validation samples indicates. After the training procedure, the weights between each neuron and the bias of each neuron were obtained. Performance of the neural network (3-10-3) is shown in Figure 3.

The improved weights of the neural network based on least mean square error are presented in Table 4. Table 4 gives the weights of the correlation between the input and the hidden layers. It also presents the weights of the correlation between the hidden and the output layers.

Testing samples are not considered during training and so provide an independent measure to validate performance of the derived network.

4 Results and discussion

Figures 4–6 shows comparison of experimental results and ANN predictions, respectively, for cutting force components Fp, Fc and Fa. The predicted ANN output values are very close to experimental measured data. The adequacy of the developed ANN models has been verified through R^2 value. The quantity R^2, also called coefficient

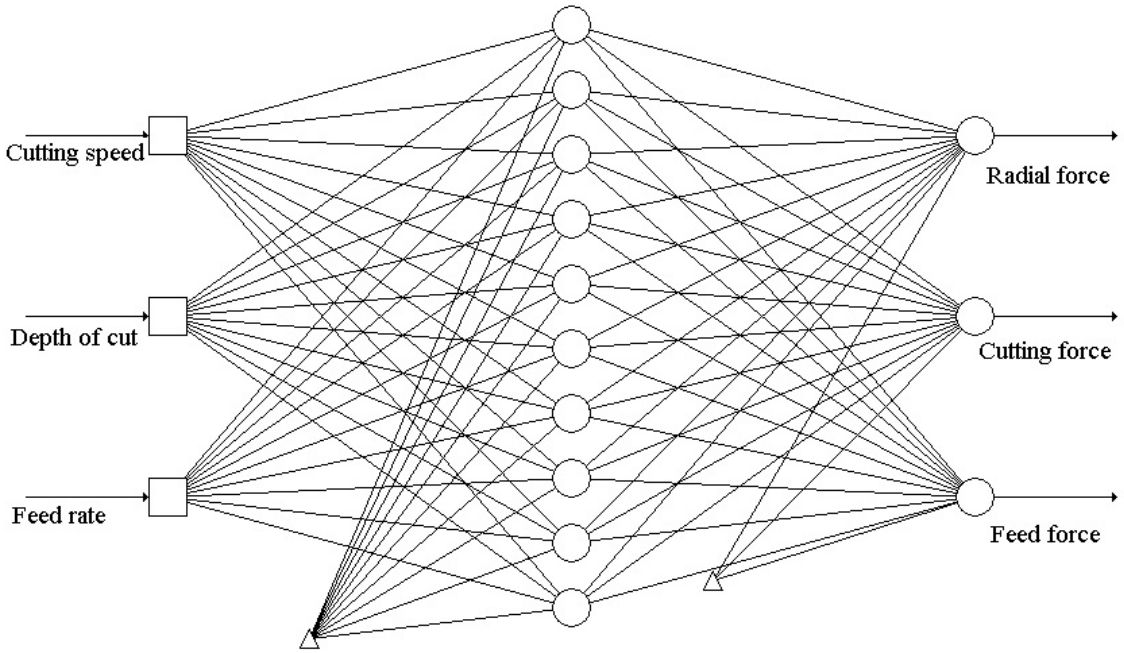

Fig. 2. Structure of the ANN for predicting the surface roughness parameters by vision system.

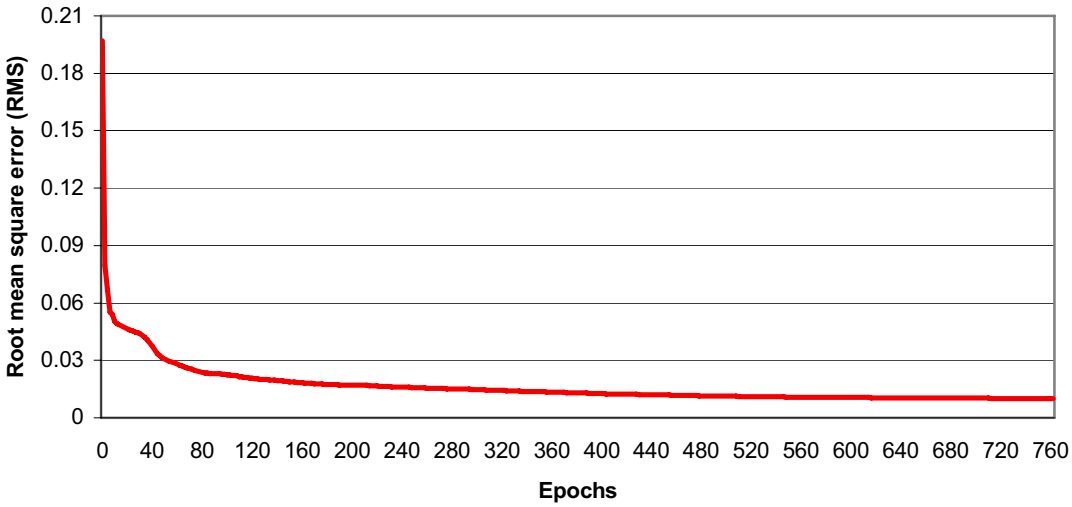

Fig. 3. Performance of the neural network structure (3-10-3).

of determination, is used to judge the adequacy of regression models. Here it was found that the coefficient of determination is equal to 99% for both roughness parameters. This shows that there exists a high correlation between the experimental results and model predicted values. To further test the validity of the derived ANN model, six verification tests were conducted at different selected conditions using the set of parameters presented in Table 5. The experimental results collected from this set of complementary tests were compared then with the model predictions.

ANN model has been run using the trained data. The graphs giving predicted and tested values are plotted in Figures 7–9. The results indicate that the built ANN model succeeded in predicting satisfactorily the cutting force components Fp, Fc and Fa as the obtained predictions are very close to experimental observations.

The cutting force decreases with an increase in cutting speed when machining Glass Fiber Reinforced Plastics (GFRP) and Carbon Fiber Reinforced Plastics (CFRP), respectively. Further experimental studies in [19] supported these results and showed that the cutting speed only slightly affects the cutting forces when machining GFRP with different tool materials and geometries. However, it was shown in [20] that the cutting forces increase with an increase in cutting speed. The rate of change of the cutting forces with cutting speed is believed to be associated with the cutting temperatures. It has been described that the cutting forces for Polycristalline diamond (PCD) are lower than those for Cemented Carbide

Table 4. The weight values connected in between the neurons of the hidden layer and output layer.

From the input layer				
to the 1th hidden layer	bias	1th neuron	2th neuron	3th neuron
1th neuron	−1.11	0.19	−2.55	0.26
2th neuron	4.15	−3.43	−3.09	−1.42
3th neuron	−0.94	−0.63	−4.94	1.67
4th neuron	−1.71	1.09	0.41	0.35
5th neuron	−0.07	−0.76	0.73	−3.80
6th neuron	−0.97	1.09	1.86	1.27
7th neuron	0.18	−2.96	1.14	1.39
8th neuron	−1.86	−0.66	−1.22	−0.99
9th neuron	−1.71	−0.66	−4.37	1.69
10th neuron	−0.44	1.58	2.54	−1.81

From the 1th hidden layer											
to the output layer	bias	1th neuron	2th neuron	3th neuron	4th neuron	5th neuron	6th neuron	7th neuron	8th neuron	9th neuron	10th
1th neuron	0.33	0.01	2.60	−0.97	−0.38	−2.07	1.57	1.01	1.30	−2.91	−2.86
2th neuron	0.54	−2.48	1.33	−1.49	−0.95	−0.50	1.96	0.72	−1.34	−1.22	−1.49
3th neuron	0.15	−0.91	0.63	−1.78	0.99	−1.37	2.08	1.14	0.97	−1.22	−1.89

Table 5. The parameters setting of verification tests showing surface roughness parameters results.

Exp. No.	Vc (m.min^{-1})	d (mm)	f (mm.rev^{-1})	Radial force Fp (N)	Cutting force Fc (N)	Feed force Fa (N)
1	300	1.5	0.1	57.87	87.70	68.16
2	300	0.25	0.1	62.47	22.22	21.55
3	200	1.5	0.1	89.62	116.70	73.67
4	200	0.25	0.1	67.52	23.65	23.61
5	100	1.5	0.1	98.94	123.86	78.75
6	100	0.25	0.1	76.86	25.19	26.93

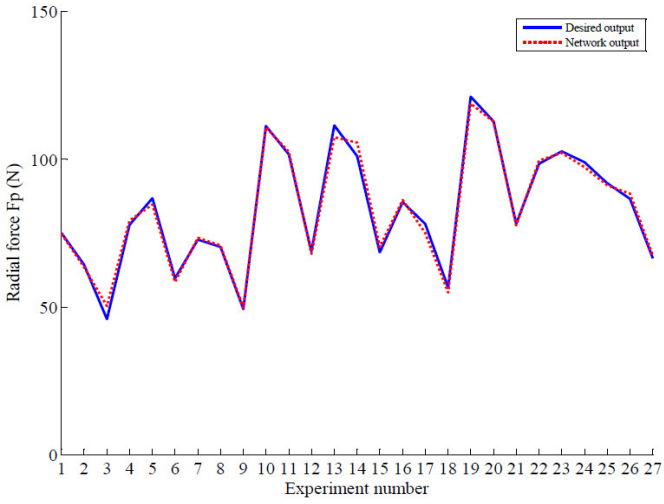

Fig. 4. Comparison of estimated and experimental results for Fp.

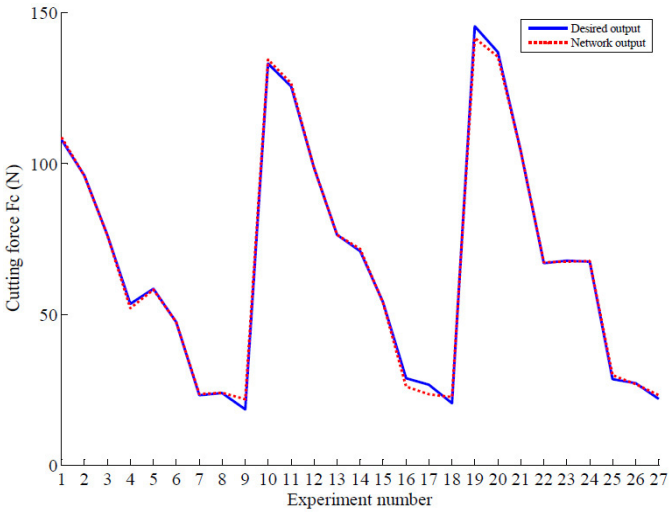

Fig. 5. Comparison of estimated and experimental results for Fc.

(K15) when machining GFRP, especially at large feed rates, and that the cutting force is critically dependent on fiber orientation, as determined by the winding angle in filament wound tubes. The cutting force increases with increasing winding angle up to 15° and decreases with further increase in winding angle. There are only a limited number of studies on effect of clearance angle on tool forces [21,22]. This work generally indicates that an increase in the clearance angle leads to slight decrease in the cutting force. It has been pointed out that for a small depth of cut as compared to the nose radius much of the material in the cutting edge path is pressed under the clearance face and then bounces back once the tool has passed [23]. Table 6 shows the sensitivity analysis for the input parameters considered. From Table 6, it can be asserted that the depth of cut is the highly influential parameter followed by feed rate for cutting force components during the machining of PEEK CF30.

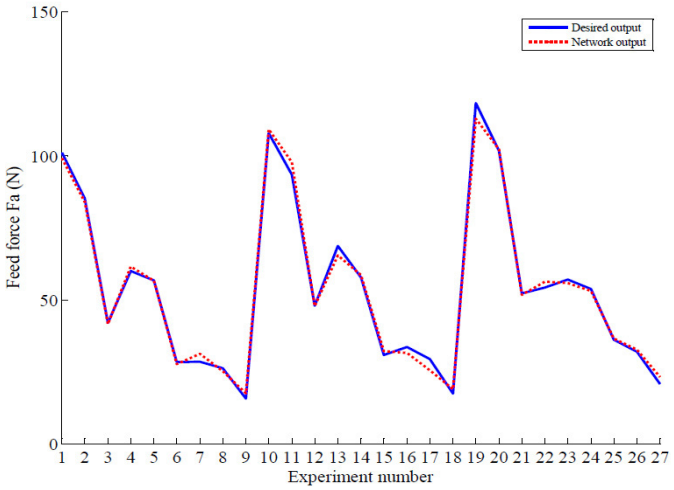

Fig. 6. Comparison of estimated and experimental results for Fa.

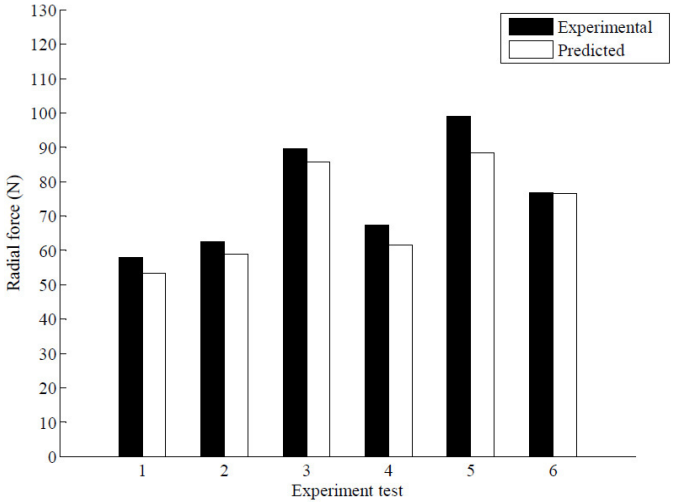

Fig. 7. Validation of ANN model for radial force Fp.

Table 6. Sensitivity of input parameters considered.

Parameters considered	Levels	Sensitivity	Diagram
d (mm)	0.25–1.5	0.19	
f (mm.rev^{-1})	0.05–0.2	0.15	
Vc (m.min^{-1})	100–300	0.03	Cutting force

5 Conclusion

Extensive experiments on the machining of PEEK CF30 with TiN coated tools were conducted. The parameters considered for the experimentation were cutting speed ranges, feed rate, and depth of cut. Back propagation Artificial Neural Network has been used to predict the cutting force components. Neural network configuration was optimized and 3-10-3 network was trained using 27 patterns to achieve the best modeling. The neural network based models have shown close matching between predicted outputs and directly measured cutting force components. Validity of these ANN models was further

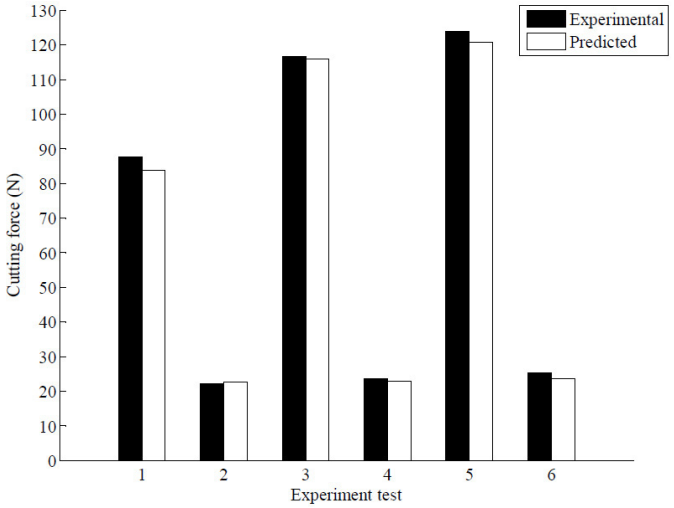

Fig. 8. Validation of ANN model for cutting force Fc.

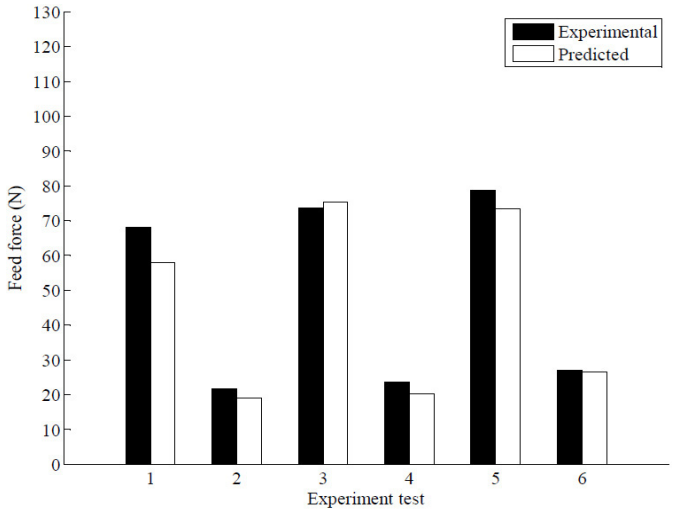

Fig. 9. Validation of ANN model for feed force Fa.

assessed by considering additional complementary tests. ANN based models have succeeded in giving always accurate estimations of experimental results. This indicates that ANN modeling is efficient in the context of predicting machining criteria for PEEK composite materials. The training of the network uses 27 data sets and the testing uses 6 data sets. The number of test data used in this work is limited. Further increase of test data will improve the results. ANN models can be used to make accurate predictions that could be beneficially used to enhance practical cutting conditions. The influence of machining parameters on the cutting force components was evaluated using a sensitivity analysis. The results indicated that the depth of cut is the most influential parameter followed by feed rate. Although the mathematical tools have been used for analysis, the objective of the research and the conclusions drawn are technological, meaning it's quite useful to manufacturing engineers involved in machining.

References

[1] F.M. Cabrera, I. Hanafi, A. Khamlichi, A. Jabbouri, M. Bezzazi, Sur l'usinabilité des composites à matrices polymères renforcée par des fibres, Mécanique & Industries 11 (2010) 93–103

[2] J.P. Davim, P. Reis. Multiple regression analysis (MRA) in modeling milling of glass fibre reinforced plastics (GFRP), Int. J. Manuf. Technol. Manag. 6 (2004) 85–197

[3] W. Konig, Wulf Ch., P. Grab, H. Willerscheid, Machining of Fibre Reinforced Plastics, CIRP Ann. 34 (1985) 537–548

[4] F.M. Cabrera, I. Hanafi, A. Khamlichi, A. Jabbouri, M. Bezzazi, Prédiction de la force d'usinage lors du chariotage du polyétheré thercétone (PEEK) CF30 en utilisant la méthode de surface de réponse, Can. Aeronaut. Space J. 57 (2011) 1–11

[5] S.A. Hussain, V. Pandurangadu, K. Palanikumar, Machinability of glass fiber reinforced plastic (GFRP) composite materials, Int. J. Eng. Sci. Technol. 3 (2011) 103-118

[6] J.P. Davim, Machining: Fondamentals and recent advances. Springer, London, 2008

[7] A. Pramanik, L.C. Zhang, J.A. Arsecularatne, Prediction of cutting forces in machining of metal matrix composites, Int. J. Machine Tools Manuf. 46 (2006) 1795–1803

[8] G. Venu Gopala Rao, P. Mahajan, N. Bhatnagar, Micromechanical modeling of machining of FRP composites - Cutting force analysis, Compos. Sci. Technol. 67 (2007) 579–593

[9] U.A. Dabade, D. Dapkekar, S.S. Joshi, Modeling of chip tool interface friction to predict cutting forces in machining of Al/SiCp composites, Int. J. Machine Tools Manuf. 49 (2009) 690–700

[10] D. Kalla, J. Sheikh Ahmad, J. Twomeya, Prediction of cutting forces in helical end milling fiber reinforced polymers, Int. J. Machine Tools Manuf. 50 (2010) 882–891

[11] S. Sikder, H.A. Kishawy, Analytical model for force prediction when machining metal matrix composite, Int. J. Mech. Sci. 59 (2012) 95–103

[12] G.R. Johnson, W.H. Cook, A constitutive model and data for metals subjected to large strains, high strain rates and high temperatures. Proceedings of the 7th International Symposium on Ballistics. The Hague. Netherlands, 1983, pp. 541–547

[13] C.C. Tsao, H. Hocheng, Evaluation of thrust force and surface roughness in drilling composite material using Taguchi analysis and neural network, J. Mater Process. Technol. 203 (2008) 342–348

[14] R. Mishra, J. Malik, I. Singh, J.P. Davim, Neural network approach for estimating the residual tensile strength after drilling in uni-directional glass fiber reinforced plastic laminates, Mater. Design. 31 (2010) 2790–2795

[15] F. Mata, I. Hanafi, E. Beamud, A. Khamlichi, A. Jabbouri, Modelling of machining force components during turning of PEEK CF30 by TiN coated cutting tools using artificial intelligence, Int. J. Machining and Machinability of Materials 11 (2012) 263–279

[16] G. Taguchi, Introduction to Quality Engineering. Publisher: Productivity Press Inc. Asian productivity organization, 1990

[17] Y. Sahin, A. Riza Motorcu, Surface roughness model for machining mild steel with coated carbide tool, Mater. Design 26 (2005) 321–326

[18] C.T. Su, J.T. Wong, S.C. Tsou, A process parameters determination model by integrating artificial neural network and ant colony optimization, J. Chinese Inst. Industrial Engineers 22 (2005) 346–354

[19] T. Kaneeda, CFRP cutting mechanism, Trans. North Am. Manuf. Res. Inst. SME 19 (1991) 216–221

[20] M. Alauddin, I.A. Choudhury, M.A. El Baradie, M.S.J. Hashmi, Plastics and their machining: A review, J. Mater. Process. Technol. 44 (1995) 40-47

[21] A. Koplev, A. Lystrup, T. Vrom, The cutting process, chips, and cutting forces in machining CFRP, Composites 14 (1983) 371–376

[22] D.H. Wang, M. Ramulu, D. Arola, Orthogonal cutting mechanisms of graphite/epoxy composite. Part I: Unidirectional laminate, Int. J. Machine Tools Manuf. 35 (1995) 1623–1638

[23] X.M. Wang, L.C. Zhang, An experimental investigation into the orthogonal cutting of unidirectional fiber reinforced plastics, Int. J. Machine Tools Manuf. 43 (2003) 1015–1022

[24] I. Hanafi, A. Khamlichi, F.M. Cabrera, E. Almansa, A. Jabbouri, Optimization of cutting conditions for sustainable machining of PEEK-CF30 using TiN Tools, J. Clean. Prod. 33 (2012) 1–9

[25] I. Hanafi, A. Khamlichi, F.M. Cabrera, P.J. Nuñez López, A. Jabbouri, Fuzzy rule based predictive model for cutting force in turning of reinforced PEEK composite, Measurement 45 (2012) 1424–1435